High-sensitivity pump-probe spectroscopy with a dual-comb laser and a PM-Andi supercontinuum

Gruber, Christoph ; Pupeikis, Justinas ; Camenzind, Sandro L ; Willenberg, Benjamin ; Camargo, Franco V A ; Lang, Lukas ; Hamm, Peter ; Rampur, Anupamaa ; Heidt, Alexander ; Phillips, Christopher R ; Cerullo, Giulio ; Keller, Ursula

DOI: https://doi.org/10.1364/ol.538105

Optics Letters

High-sensitivity pump-probe spectroscopy with a dual-comb laser and a PM-Andi supercontinuum

Christoph Gruber,[1,†] Justinas Pupeikis,[1,†,*] Sandro L. Camenzind,[1] Benjamin Willenberg,[1] Franco V. A. Camargo,[2] Lukas Lang,[1] Peter Hamm,[3] Anupamaa Rampur,[4] Alexander Heidt,[4] Christopher R. Phillips,[1] Giulio Cerullo,[2,5] and Ursula Keller[1]

[1]Department of Physics, ETH Zurich, 8093 Zurich, Switzerland
[2]Istituto di Fotonica e Nanotecnologie, Consiglio Nazionale delle Ricerche, 20133 Milano, Italy
[3]Department of Chemistry, University of Zurich, 8057 Zurich, Switzerland
[4]Institute of Applied Physics, University of Bern, 3012 Bern, Switzerland
[5]Dipartimento di Fisica, Politecnico di Milano, 20133 Milano, Italy
[†]These authors equally contributed to this work.
[*]pupeikis@phys.ethz.ch

Received 1 August 2024; revised 11 October 2024; accepted 21 October 2024; posted 21 October 2024; published 6 November 2024

Amplifier-based pump-probe systems, while versatile, often suffer from complexity and low measurement speeds, especially when probing samples require low excitation fluences. To address these limitations, we introduce a pump-probe system that leverages a 60-MHz single-cavity dual-comb oscillator and an ultra-low noise supercontinuum. The setup can operate in equivalent time sampling or in programmable optical delay generation modes. We employ this system to study the wavelength-dependent excited-state dynamics of the non-fullerene electron acceptor Y6, a compound of interest in solar cell development, with excitation fluences as low as 1 nJ/cm^2, well below the onset of nonlinear exciton annihilation effects. Our measurements reach a shot-noise limited sensitivity in differential transmission of $3.4{\cdot}10^{-7}$. The results demonstrate the system's potential to advance the field of ultrafast spectroscopy.

https://doi.org/10.1364/OL.538105

Ultrafast optical spectroscopy is a powerful tool for characterizing the non-equilibrium optical response of samples, including biomolecules, organic and inorganic substances and hybrid semiconductors [1]. Among the different available techniques, the most widespread is pump-probe spectroscopy, in which a first pump pulse excites the sample, and a second time delayed probe pulse measures the differential transmission ($\Delta T/T$) or reflection ($\Delta R/R$). Often pump-probe spectroscopy is combined with microscopy, thereby retrieving simultaneously the spatial and temporal information [2–5]. The rich physics of these diverse samples requires versatile multi-color light sources, to be able to excite different optical transitions and probe the spectral signatures of the photoexcited species.

Typical pump-probe setups are based on amplified laser systems, which consist of a femtosecond oscillator and a laser amplifier, producing pulses with μJ-to-mJ energy and 1–100 kHz repetition rate, possibly followed by optical parametric amplifiers to tune the pump and/or probe wavelength. In these setups, the pump-probe delay is typically scanned using a mechanical delay line [6]. Such systems are generally complex and challenging to integrate into cost-effective microscopy setups. Additionally, the reduced pulse repetition rate in amplified systems lowers the sampling rate, reducing the sensitivity and potentially limiting imaging applications.

An alternative approach to pump-probe systems is to use only oscillators, resulting in sources with higher repetition rate $f_{rep} \approx 100$ MHz and moderate pulse energies of a few tens of nanojoules. Using a pair of oscillators with a slight repetition rate difference Δf_{rep} is a convenient way to enable rapid optical delay scans, as the time delay between subsequent pulse pairs is continuously swept. In this equivalent time sampling (ETS) approach [7], also referred to as asynchronous optical sampling (ASOPS) [8], features with characteristic frequencies in the THz range are scaled by the ratio $\Delta f_{rep}/f_{rep}$ down to the electronically accessible MHz range. This frequency range, in comparison to DC, is beneficial since the signal noise is then dominated by the detector shot noise, thus allowing to achieve an ultra-low noise floor. However, ETS systems typically employ two oscillators emitting at the same wavelength, so that pump and probe pulses are degenerate. To achieve independent tunability of pump and probe wavelengths and low noise operation, it is usually necessary to deploy more complex systems based on Ti:sapphire lasers or optical parametric oscillators [9,10]. A further issue with ETS systems is that they inherently scan the optical delay between the pulses over a range $1/f_{rep} \approx 10$ ns, which may be too large for certain applications.

In this work, we leverage two recent innovations: the development of polarization-maintaining all-normal dispersion (PM-ANDi) microstructured fibers compatible with ultra-low noise

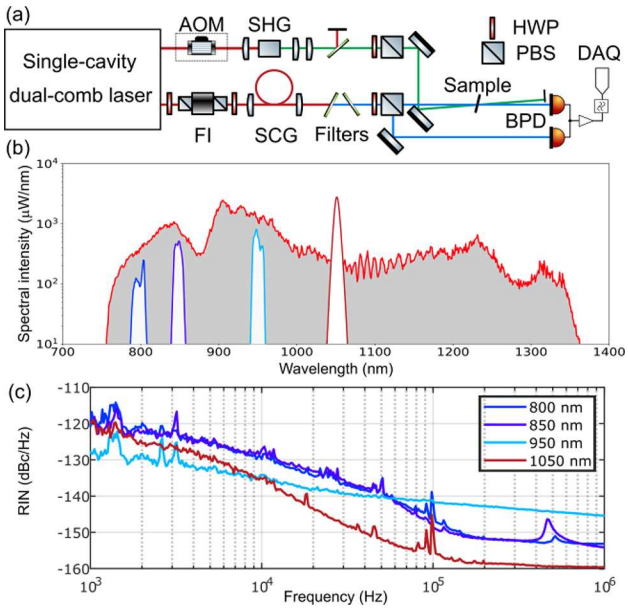

Fig. 1. (a) Experimental setup. AOM, acousto-optic modulator (only for the programmable delay experiment); SHG, second harmonic generation; HWP, half-wave plate; PBS, polarizing beam splitter; SCG, supercontinuum generation; FI, Faraday isolator; BPD, balanced photodetector; DAQ, digitizer. (b) Probe spectrum as obtained directly from the oscillator, after PM-ANDi fiber and few selected slices after spectral filtering. (c) Relative intensity noise (RIN) power spectral density for selected bands of the supercontinuum and the oscillator (1050 nm).

supercontinuum generation [11], and dual-comb bulk solid-state lasers implemented in a single-cavity with a biprism approach [12]. Combining these technological advances, we present a simple, yet high-performance multi-color pump-probe system based on ETS, scanning an optical delay of 16.6 ns, from a 60-MHz pulse repetition rate, at speed up to 1 kHz. We also implement programmable optical delay generation of the oscillator via an electronic feedback loop that uses time-to-digital converters (TDCs) to measure the delay between the two pulse trains [13]. We finally apply this multi-color pump-probe system to study the non-fullerene electron acceptor (NFA) Y6, a compound of significant interest in organic solar cell development [14]. We characterize the sample's behavior at fluences as low as 1 nJ/cm^2, for which nonlinear effects due to many-body kinetics are negligible.

Figure 1(a) shows the experimental layout. Given the low fluence on the sample and the need to measure at multiple probe wavelengths, the supercontinuum noise needs to be sufficiently low to resolve small ΔT/T signals. Recent research has explored PM-ANDi supercontinuum for oscillator-based pump-probe applications [15,16]. However, to our knowledge, it has not been used in ETS configurations.

We address the need for two lasers in the ETS approach by using a single-cavity dual-comb laser system in which both lasers share the same cavity arrangement, thereby simplifying the system hardware considerably. The laser system, similar to the one reported in [12,17], is a spatially multiplexed (via a biprism) solid-state laser delivering 2.2 W of average power per pulse train at a center wavelength of 1050 nm. The biprism is mounted on a piezoelectric stage which allows fine control of the repetition rate difference Δf_{rep}. For the ETS experiment Δf_{rep} was set to 600 Hz, and the sum-frequency generation coincidence signal served as signal acquisition trigger and Δf_{rep} drift stabilization signal.

One beam (pump) has been frequency-doubled in a 5-mm-long lithium triborate (LBO, $\theta = 90°$, $\varphi = 12.6°$) crystal. The second harmonic was collimated by a pair of cylindrical lenses to compensate for the beam ellipticity due to the spatial walk-off in the LBO. The second harmonic generation efficiency was 50%.

The other output beam (probe) was spectrally broadened in a 20-cm-long PM-ANDi fiber. We used NL-PM-1050-NEG (NKT Photonics) fiber with collapsed air-holes to increase the coupling efficiency. We could obtain 54% coupling efficiency in the nonlinear fiber. A Faraday isolator was included to mitigate backreflection from the fiber tip. Because of the isolator dispersion, the pulse duration at the fiber input was 186 fs, based on a second-harmonic autocorrelation measurement. A half-wave plate before the PM-ANDi was used to find the lowest noise point. Spectral filtering of the supercontinuum was realized by a combination of bandpass and shortpass filters (from a set of FESH1000, FL850-10, FBH1050-10, Thorlabs) to select ~10-nm-wide spectral slices. The probe wavelength was fine-tuned by tilting the bandpass filters. The obtained supercontinuum spectrum and few representative spectral slices are shown in Fig. 1(b).

An important feature of driving the PM-ANDi supercontinuum generation with bulk solid-state lasers is that the resulting source can have ultra-low relative intensity noise (RIN) at the shot-noise level even after spectral filtering, as demonstrated recently in a related work using a gigahertz dual-comb pump laser [18]. In that study the spectral filter was implemented with a monochromator, which would be an alternative to the discrete filters used in this work. Compared to [18], the 60-MHz laser used here has >10 times as much pulse energy available and about twice as long pulse duration. Hence, it supports more self-phase-modulation in the fiber, which leads to a broader output spectrum but also to more noise, particularly around the central wavelength [19]. Accounting for this trade-off, the supercontinuum generation was performed with 300 mW of average power inside the nonlinear fiber, corresponding to 24 kW of peak power. The obtained optical bandwidth covers the range 770 to 1320 nm (−10 dB). Although peak powers up to 90 kW (in the fiber) were available, and a broader optical bandwidth could be generated, we observed that the RIN of the spectrally filtered supercontinuum tended to degrade above 40 kW. Additionally, higher input power did not necessarily increase the average power in the selected spectral slices.

We characterized the intensity noise and pulse duration properties of the selected spectral slices. Figure 1(c) shows the obtained RIN power spectral density, and Table 1 summarizes the results. The average power on the photodiode was adjusted with neutral density filters to obtain a comparable average photocurrent in each measurement. We observed that the 800- and 850-nm spectral slices were close to the shot-noise limit, while the 950-nm spectral slice exhibited 10 dB of excess noise. Nevertheless, the observed noise floor around 1 MHz offset frequency is >50 dB lower compared to the typical performance of the soliton-based supercontinua generated from anomalous dispersion fibers [20]. The average power per slice is on the order of a few mW, which is sufficient to act as a probe in the experiment.

The 525-nm pump beam was shaped to a relatively large 700-μm 1/e^2 radius spot to support a range of peak fluence values

Table 1. Laser and Supercontinuum Performance Summary

	Oscillator (1050 nm)	800 nm	850 nm	950 nm
Power (mW)	2200	2.2	5.3	8.2
Pulse duration (fs)	186	181	129	331
RIN at 1 MHz (dBc/Hz)	<−158	−153	−153	−145
Characterization shot-noise limit (dBc/Hz)	−158	−155	−156	−155
Average photocurrent (mA)	2.1	1	1.24	1.14

on the sample from 1 nJ/cm^2 to 1 μJ/cm^2 (0.5 to 500 mW). The probe beam size was 200 μm 1/e^2, so that it samples the peak fluence of the pump. Before reaching the sample, the probe beam was split using a half-wave plate and a polarizer into two parts: one for the sample and one for the reference signal. We used a balanced photodetector (PDB425, Thorlabs) followed by a digitizer (PCI-5122, National Instruments) for three reasons: (1) the balanced detector contains an integrated transimpedance amplifier, increasing the signal strength above our digitizer noise floor; (2) it is configured to achieve shot-noise limited performance with an average power of 0.1 to 1 mW, which is a suitable range considering the probe power loss on the sample; and (3) it allows cancellation of the oscillator's low-frequency noise.

We used our multi-color pump-probe system to study the NFA Y6 [21]. NFAs are small molecules with bandgap tunable by synthetic design which have dramatically increased the efficiency of organic solar cells, by contributing to light absorption and charge separation [22]. However, in typical pump-probe experiments with amplified systems, NFAs are excited with fluences higher than 1 μJ/cm^2, which can induce many-body kinetics and alter excitation lifetimes [23].

First, we perform ETS measurements at 800-nm probe wavelength, where we observe a positive ΔT/T signal due to ground-state bleaching (GSB), to determine the maximum pump fluence that can be used before the onset of nonlinear exciton–exciton annihilation effects. We study a Y6 NFA film deposited on a glass substrate. Because the sample is susceptible to photo-oxidation, during the experiment it is placed in a vacuum chamber. An averaging time of around 9 min per trace was chosen to obtain sufficient sensitivity for the low fluence acquisitions. The data is shown in Fig. 2(a). Starting from pump fluences as low as ≈1 nJ/cm^2 and increasing the fluence, the sample's ultrafast response does not change significantly until ≈510 nJ/cm^2 where it starts to decay faster, which can be explained by the onset of bimolecular decay processes [24]. At low pump fluences the ΔT/T signal decays to 50% of its peak value after around 230 ps, whereas at 1 μJ/cm^2 the decay occurs within 144 ps. This highlights that low excitation fluences, well below 1 μJ/cm^2, are needed to prevent many-body kinetics that are not present under natural sunlight excitation. Such low fluences are hard to reach with low repetition rate (kHz) pump-probe systems, since the signal would be deep in the noise floor.

Next, we study the sample response at different probe wavelengths. Figure 2(b) shows the observed response obtained at 800, 850, and 950 nm. The ΔT/T signal is strongest at around 850 nm, which is also close to the reported peak of the linear

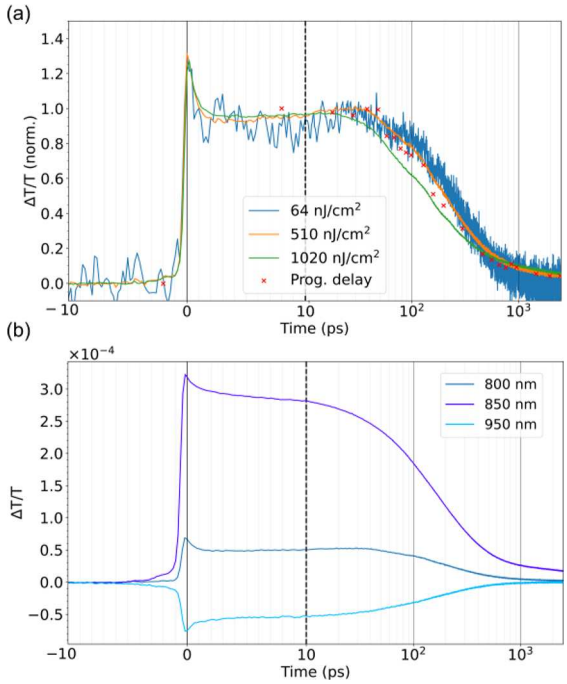

Fig. 2. (a) Lin-log represented ΔT/T dynamics in case of 525-nm pump and 800-nm probe at different fluences on the Y6 film. Data points marked by crosses indicate programmable delay pump-probe signal obtained at 1020 nJ/cm^2 pump fluence. (b) Lin-log represented ΔT/T dynamics at 510 nJ/cm^2 pump fluence at different probe wavelengths.

absorption spectrum of Y6, and where we also observe a GSB [25]. At 950 nm, on the other hand, the ΔT/T signal changes sign, and we detect a photoinduced absorption from the excited state. We observed that the rising edge of the sample response features a pedestal, likely due to electronic signal processing during data acquisition. Given a Δf_{rep} of 600 Hz, the Nyquist frequency of 30 MHz corresponds to an optical frequency of 3 THz. Therefore, a 15-MHz analog bandpass filter was included to avoid aliasing, resulting in an effective time resolution of around 666 fs.

We evaluate the measurement noise floor by calculating the standard deviation at negative delays. We found that at 850-nm probe wavelength we obtained an ultrahigh sensitivity of $3.4{\cdot}10^{-7}$ ΔT/T rms over approximately 9 min of measurement time (≈300,000 full traces) while the measurement at 950-nm had $7.5{\cdot}10^{-7}$ ΔT/T rms. The measurements at 850 and 800 nm were limited by the shot noise, while the 950-nm noise floor was affected by the elevated supercontinuum noise, suggesting that balancing was not effective, potentially due to high frequency noise, not perfect optical path difference matching or the fact that a polarizer was used to split the probe into the two beams.

The ETS mode achieved high sensitivity over the complete 16.6-ns time window, sampled at equidistant steps of 166 fs. This sampling is ideal for measurements such as picosecond ultrasonics [17]. However, many pump-probe processes exhibit an exponential decay, where logarithmic temporal sampling could be more efficient. Such sampling can be obtained by making small changes of Δf_{rep} around a nominal value of 0 Hz in order to phase-lock the delay between the two pulse trains [26]. Using lasers with low timing noise is beneficial since only jitter up to the feedback servo bandwidth can be compensated. This makes

single-cavity dual-comb lasers interesting candidates since their ultra-low relative timing jitter implies that only a slow feedback is required.

An interesting route to simplify the electronics required for programmable delay scanning is to use TDCs. We measure each comb with a 1 GHz photodiode and send the obtained signals to a custom electronics board, as reported in [13]. Based on the relative arrival time of the pulses in both combs a feedback signal acts on the biprism inside the cavity, which allows to obtain a proof-of-concept log-scale delay-sampled pump-probe signal.

To estimate the obtainable relative timing precision, we first sent the same pulse train to the two inputs of the board, which would ideally yield a constant delay since the delay between two copies of a single pulse train is measured. For relative delay sampling at 100 Hz and 1 kHz over a 10-s window, we observed standard deviations of 540 and 654 fs, respectively. As the timing measurement precision no longer improved with the square root of the number of averages, we concluded that the measurement is limited by the $1/f$ noise of the electronics. Therefore, we can expect sub-ps timing precision when setting delays, which is sufficient for most pump-probe applications including the Y6 measurements. In this case, to shift the measurement signal away from the DC, we used an acousto-optic modulator (AOM) in a single pass configuration in the pump path, modulating the pump at the AOMs fastest rate of 500 kHz. We used a 100 ms integration time per programmable delay time window. The obtained time trace matched the ETS data [Fig. 2(a)]. We collected 22 data points, which theoretically could be acquired in just a few seconds, however manual delay entry was used in this instance. The resulting time trace had a somewhat higher noise level, indicating that a more dedicated study would be needed to optimize the programmable delay pump-probe implementation. For this aspect of our work, we focused on a proof-of-concept demonstration, as pump-probe noise floor optimization with modulators is already well researched and understood [10]. If optimized, the programmable delay implementation should yield an even lower noise floor than the ETS configuration.

In summary, we demonstrated a versatile and high-performance multi-color pump-probe system combining ETS with a single-cavity dual-comb oscillator with PM-ANDi supercontinuum generation and programmable optical delay generation modes. This system achieves ultrahigh sensitivity measurements across a wide spectral bandwidth and performs rapid, long optical delay sweeps, making it exceptionally well-suited for sensitive pump-probe experiments. As an example, we demonstrate the study of an organic solar cell material under conditions relevant for practical applications, with ultra-low excitation fluences close to real-world ambient illumination. We also achieved, to our knowledge, the first demonstration of programmable optical delay generation for a single-cavity dual-comb laser. Future improvements could include implementing modulated delay sweeps around a limited time window to mitigate $1/f$ noise, similar to ECOPS [26] or MASOPS [27] approaches.

Funding. Schweizerischer Nationalfonds zur Förderung der Wissenschaftlichen Forschung (40B1-0_203709, 40B2-0_180933, PCEFP2 182222, TMPFP2 210543); Ministero dell'Università e della Ricerca (CUP B53C22001750006, ID D2B8D520, I-PHOQS, IR0000016); HORIZON EUROPE European Innovation Council (101130384, HORIZON-EIC-2023-PATHFINDEROPEN-01, QUONDENSATE, 101047137, HORIZON-EIC-2021-PATHFINDEROPEN-01, TROPHY); European Research Council (HOLOFAST, 101117858).

Acknowledgment. We thank our collaborator Prof. Dr. Patrice Camy, CIMAP of Caen, France for manufacturing the Yb:CaF_2 gain crystal used in the described laser. The authors further acknowledge support of the technology and cleanroom facility FIRST of ETH Zurich for advanced micro- and nanotechnology. We thank Prof. Nicola Gasparini and Zhuoran Qiao for providing the Y6 samples.

Disclosures. J.P., B.W., and L.L. declare partial employment at K2 Photonics AG.

Data availability. Data underlying the results presented in this paper are not publicly available at this time but may be obtained from the authors upon reasonable request.

REFERENCES

1. M. Maiuri, M. Garavelli, and G. Cerullo, J. Am. Chem. Soc. **142**, 3 (2020).
2. L. Liu, A. Viel, G. L. Saux, *et al.*, Sci. Rep. **9**, 6409 (2019).
3. C. Boule, D. Vaclavkova, M. Bartos, *et al.*, Phys. Rev. Mater. **4**, 034001 (2020).
4. T. L. Purz, B. T. Hipsley, E. W. Martin, *et al.*, Opt. Express **30**, 45008 (2022).
5. M. Hörmann, F. Visentin, A. Zanetta, *et al.*, Ultrafast Sci. **3**, 0032 (2023).
6. A. L. Dobryakov, S. A. Kovalenko, A. Weigel, *et al.*, Rev. Sci. Instrum. **81**, 113106 (2010).
7. K. J. Weingarten, M. J. W. Rodwel, and D. M. Bloom, IEEE J. Quantum Electron. **24**, 198 (1988).
8. P. A. Elzinga, R. J. Kneisler, F. E. Lytle, *et al.*, Appl. Opt. **26**, 4303 (1987).
9. B. Lomsadze and S. T. Cundiff, Science **357**, 1389 (2017).
10. M. C. Fischer, J. W. Wilson, F. E. Robles, *et al.*, Rev. Sci. Instrum. **87**, 031101 (2016).
11. A. Rampur, D.-M. Spangenberg, B. Sierro, *et al.*, Appl. Phys. Lett. **118**, 240504 (2021).
12. J. Pupeikis, B. Willenberg, S. L. Camenzind, *et al.*, Optica **9**, 713 (2022).
13. J. Helbing and P. Hamm, J. Phys. Chem. A **127**, 6347 (2023).
14. Q. Liu, Y. Jiang, K. Jin, *et al.*, Sci. Bull. **65**, 272 (2020).
15. M. Rai, W. E. Deeg, B. Lu, *et al.*, Opt. Lett. **48**, 570 (2023).
16. N. M. Kearns, A. C. Jones, M. B. Kunz, *et al.*, J. Phys. Chem. A **123**, 3046 (2019).
17. J. Pupeikis, W. Hu, B. Willenberg, *et al.*, Photoacoustics **29**, 100439 (2023).
18. S. Camenzind, B. Sierro, B. Willenberg, *et al.*, "Shot-noise limited dual-comb supercontinuum," Optica Open 112418 (2024).
19. A. Heidt, J. Feehan, J. H. V. Price, *et al.*, J. Opt. Soc. Am. B **34**, 764 (2017).
20. K. L. Corwin, N. R. Newbury, J. M. Dudley, *et al.*, Phys. Rev. Lett. **90**, 113904 (2003).
21. Y. Yang, ACS Nano **15**, 18679 (2021).
22. J. Hou, O. Inganäs, R. H. Friend, *et al.*, Nat. Mater. **17**, 119 (2018).
23. J. Piris, T. E. Dykstra, A. A. Bakulin, *et al.*, J. Phys. Chem. C **113**, 14500 (2009).
24. J. Shi, A. Isakova, A. Abudulimu, *et al.*, Energy Environ. Sci. **11**, 211 (2018).
25. J. Yuan, Y. Zhang, L. Zhou, *et al.*, Joule **3**, 1140 (2019).
26. F. Tauser, C. Rausch, J. H. Posthumus, *et al.*, in *Commercial and Biomedical Applications of Ultrafast Lasers VIII*, Vol. 6881 (SPIE, 2008), pp. 139–146.
27. M. C. Velsink, M. Illienko, P. Sudera, *et al.*, Rev. Sci. Instrum. **94**, 103002 (2023).